

Photodiode measurements in Nucte-II

M. Machida* and E. A. Aramaki**

Instituto de Física, Universidade Estadual de Campinas, Caixa Postal 6165, Campinas, 13081, SP, Brasil

and

T. Takahashi, M. Ohara and Y. Nogi

College on Science and Technology, Nihon University, Tokyo, Japan

Received on September 22, 1988

Abstract Direct measurements of light emission from plasma produced by a field reversed theta-pinch **NUCTE-II** have been performed by using a set of photodiode detectors. The analysis shows that the plasma light emission can be related to the **bremsstrahlung** radiation and it is used to identify $n = 2$ rotational instability parameters as rotation direction, angular velocity, and radial and **axial** displacement of the plasma **column**. A rough **estimate** for the temporal behaviour of the electron temperature has **also** been obtained by **using** the photodiode signal together with He-Ne laser interferometer and flux excluded signals.

1. Introduction

Theta-pinch machines have been operating in **many** places for some decades. A particular version of this machine, **namely** the field reversed configuration (FRC) type, is currently the preferred one and **several** advances have been reported in recent **years**^{1,2,3}. This configuration produces compact toroidal plasmas with very large aspect ratio and small or zero toroidal magnetic field, which usually display an $n = 2$ rotational instability during the first **30 μ s** of their equilibrium **phase**^{3,4}.

* Present address: Instituto de Física, Universidade de São Paulo, Caixa Postal 20516, São Paulo, 01498, SP, Brasil.

** (PICD) Departamento de Física e Química, Faculdade de Engenharia de Guaratinguetá, Universidade Estadual **Paulista** "Júlio de Mesquita Filho".

This instability deforms the plasma column elliptically until it reaches the wall of the discharge tube and destroys the plasma confinement. Although instability suppression techniques for this $n = 2$ instability have already been successfully used, it still is the subject of continuing investigation as its origins are not yet fully understood^{3,4,5}.

This instability can be monitored in many ways, such as laser interferometry and light emission analysis with a spectrometer or with photodiode arrays⁶. Among these, photodiode arrays are the cheapest and the most straightforward diagnostic tool.

In this paper we present the results of photodiode array measurements taken in NUCTE-II⁷. This diagnostic technique can measure precisely the continuum light emission from the plasma and indicates clearly when deformation of the column due to the $n = 2$ instability begins, as the light emission is modulated by the deformation. Furthermore, when coupled with interferometric and external magnetic probe data, this technique allows the electron temperature to be estimated. Also the rotational velocity and the approximate radial and axial size of the plasma column can be inferred from these measurements.

This technique can be further used in other machines, as in USP's small tokamak TBR-I⁸, where the bremsstrahlung radiation is confirmed by X-ray diagnostics and the plasma body is dominated by mode oscillations⁹.

NUCTE-II produces a FRC plasma via a theta-pinch discharge with reversed bias in which a small toroidal field is generated by an internal axial current discharge. A schematic drawing of the machine is shown in fig.1. The full length and inner diameter of the solenoid coil are 170 cm and 6 cm respectively. The vacuum vessel is made of quartz and is evacuated to a base pressure of 2 to 4×10^{-7} Torr by a turbomolecular pump. Deuterium gas is used at 12 mTorr in a 14 cm discharge tube. NUCTE-II has a 24 kJ slow bank and a 54 kJ fast bank for the main compression field. The plasma is preheated with an oscillating discharge of axial current I_{z1} of 35 kA peak value as shown in fig. 2. When the negative bias field reaches a value of - 630 G the main compression is fired with rise time, peak field value, and e-folding time of 2 μ s, 12 kG, and 65 μ s, respectively. A second discharge

Photodiode measurements in Nucte-II

of the internally applied axial current, I_{z2} , is used to study the enhancement of the trapped flux and the effects of a weak toroidal field on the equilibrium phase. Further details on the parameters and the operation of the machine are presented elsewhere⁷.

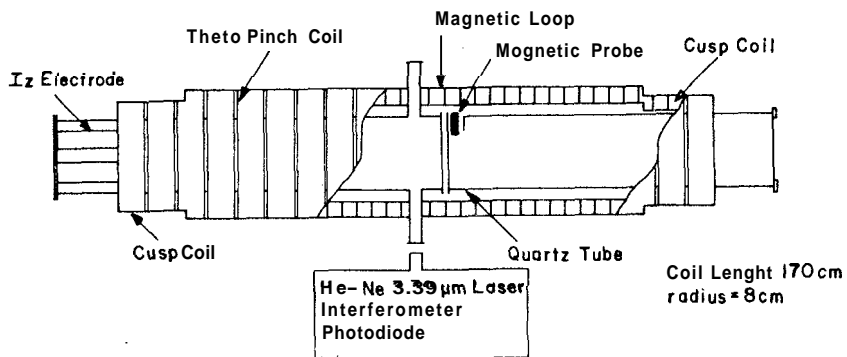


Fig.1 - Experimental apparatus of NUCTE-II.

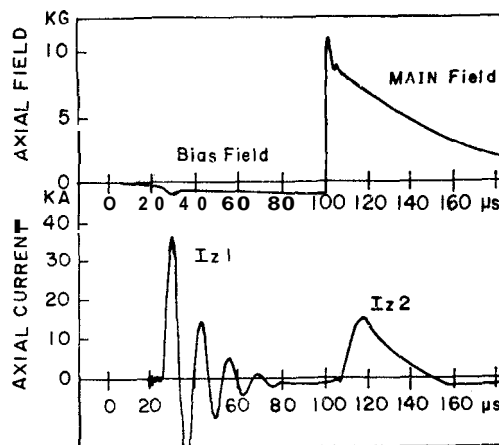


Fig.2 - Time sequence of axial field and current.

2. Experimental results

In this section we analyse the data obtained with a photodiode array in the visible region. The $n = 2$ instability is clearly seen and comparison with other diagnostics. He-Ne laser interferometry and excluded flux probes, shows that this technique is a good, reliable, routine diagnostic tool, easy to **install** and to **operate**. Fig.3 shows the photodiode set up together with a typical discharge signal, where the $n = 2$ instability appears clearly $25\mu\text{s}$ into the equilibrium phase. All the photodiodes used in the array are from EG & G, type **SGD - 100 A**.

The light emitted from the plasma and captured by the photodiode array can be thought of as originating from two regions: (1) from the whole plasma body along the radial line of sight, or (2) from a thin layer on the **surface** of the plasma **column**. With the **assumption** that **all** elementary plasma volume are light emitters of equal intensity, these two hypotheses can be distinguished by an analysis of the length of the region (ta) which emits the light captured by the photodiodes. Also, **assuming** the plasma to be a rotating elliptical rigid body, as in the $n = 2$ instability phase, with an **eccentricity** $E = b/a$ and equivalent area radius $r, = (a/b)^{1/2}$, the variation of the emission length ta as a function of the rotating angle θ can be plotted as shown in fig. 4. The continuous line **represents** the case of light emitted from the whole plasma volume, and the dotted line the case of emission from a thin **external** layer of thickness $H = 0.2$.

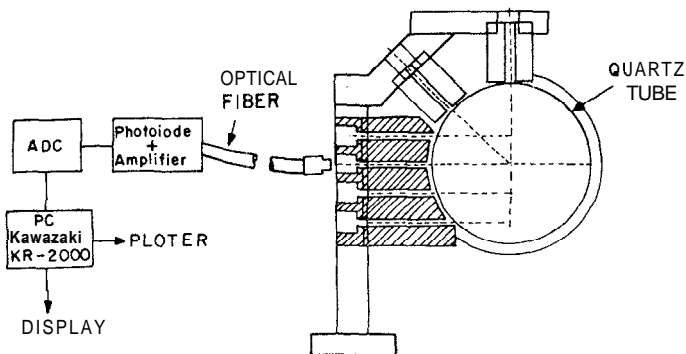


Fig.3.A - Photodiode sensor setup and collection system.

Photodiode measurements in Nuete-11

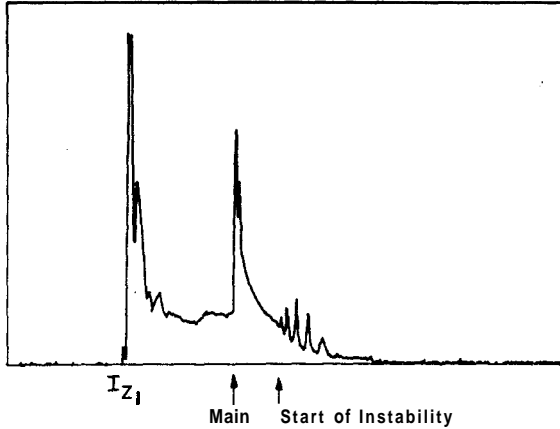


Fig.3.B - Typical photodiode signal with $N = 2$ instability (full scale $400 \mu s$).

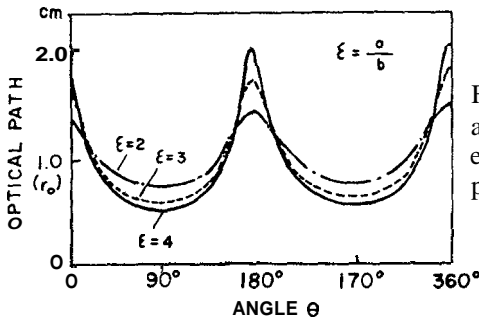


Fig.4.A - Variation of optical path against θ of rotating rigid body with elongation $\epsilon = a/b$ for line integrated plasma.

Comparison of this figure with the experimental photodiode signals in the instability interval, as in fig. 5, leads to the conclusion that the light captured by the photodiode comes from the whole plasma body and not from a thin **surface** layer. (The experimental data do not have the dip at the peak of the curve **and** the upper and lower peaks of instability are very similar to theoretical results). Note that the growth of the instability was ignored in our analysis for the sake of simplicity. Therefore we can associate the photodiode signals with an elliptically deformed plasma column of major and minor **axis** a and b .

The separatrix radius r , can be determined as a function of time, while the instability is present, by taking the r , as $r = (ab)^{1/2}$ and a (and b) are read from

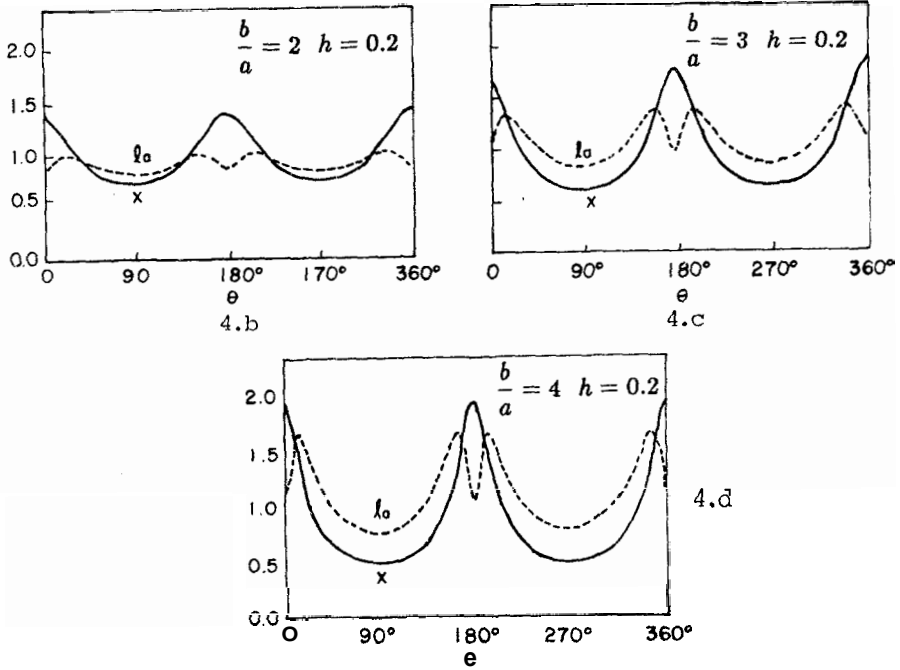


Fig.4.B, C, D - Variation of optical path against θ of rotating rigid body for surface emission with different elongation.

the upper (and lower) intensity values taken from the photodiode signal. The equivalent r_c value is also plotted in the fig. 5. Furthermore a comparison can be made with the data from a He-Ne $3.39\mu\text{m}$ laser interferometer. Since both diagnostics represent line integrated signals, they should represent the same kind of behavior, and this is indeed seen in fig. 6. The 180° phase difference seen there is due to the 90° difference in the radial position of each detector.

The light detected by the photodiode can be thought of as continuum light emission by bremsstrahlung radiation, which in the semiclassical treatment is given by¹⁰

$$W(P)d\nu \approx 6.3 \cdot 10^{-53} Z^2 \left(\frac{1}{T_e}\right)^{1/2} n_e n_i \exp\left(-\frac{h\nu}{T_e}\right) d\nu (W/m^3) \quad (1)$$

where the term on the left is the power radiated per unit volume of plasma between the frequencies ν and $\nu + d\nu$, and T_e is given in eV. For the case of $n_e \approx n_i, Z_i = 1$

Photodiode measurements in Nucte-II

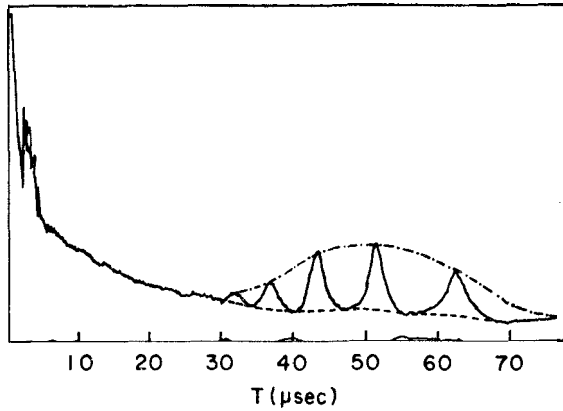


Fig.5.A - Typical photodiode signal with plotting of enveloped upper and lower curves, ($T=0$ for main bank start time).

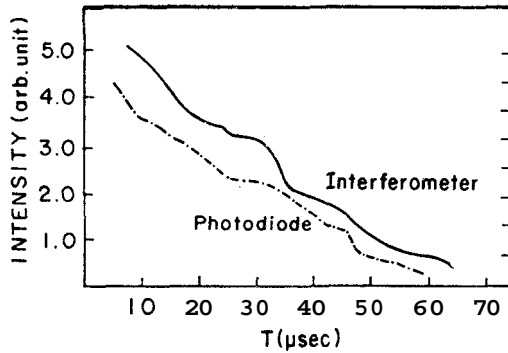


Fig. 5.B - Time dependence for photodiode and interferometer signal using geometric average values for envelope region.

(deuterium plasma) and $h\nu \ll kT_e$, the above equation can be rewritten in the form of a line integrated intensity as

$$I = An^2 r_e T^{1/2} \tag{2}$$

and here n is the electron density, r_e the separatrix radius, T is the electron temperature in electron volts and A is a calibration constant.

In order to compare eq.(2) with the photodiode signals, the time variation of the density, the separatrix radius and the electron temperature are needed. They

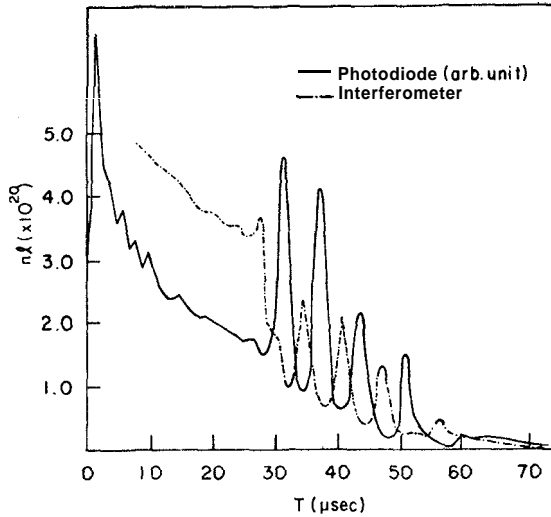


Fig.6 - Comparison between interferometer and photodiode signal.

can be obtained from other diagnostics such as interferometer data for n_e and flux excluded signals for r ; the temperature dependence can be obtained from

$$\langle \beta \rangle = 1 - \frac{1}{2} \left(\frac{r_e}{r_w} \right)^2 \quad (3)$$

where r_e is the radius of the quartz wall and

$$\langle \beta \rangle = \frac{nk \langle T \rangle}{B_{ext}^2 / 2\mu_0}$$

We have then

$$\langle T \rangle = \frac{B_{ext}^2}{2\mu_0} \frac{1}{nk} \left(1 - \frac{1}{2} \frac{r_e^2}{r_w^2} \right) \quad (4)$$

and all quantities on the RHS are known. The plots of n_e , r , B_{ext} and T versus time are shown in fig. 7. These values are then used in eq.(2) and the light intensity is obtained as a function of time, within the assumption that the emission comes from bremsstrahlung radiation.

Photodiode measurements in Nucte-II

This function is plotted together with the photodiode signals in fig. 8. The agreement is remarkable and the differences **seen**, mainly in the unstable region, are probably due to the use of an average temperature in **eq.(2)**.

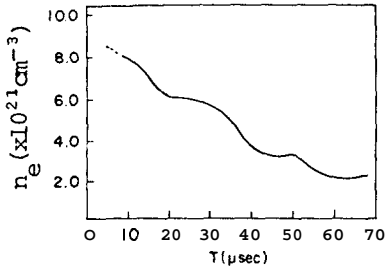


Fig. 7.A - N_E value from interferometry.

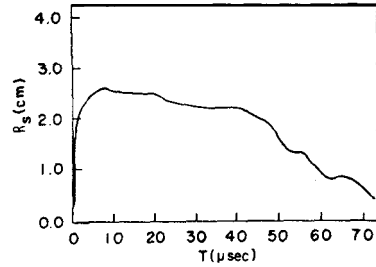


Fig. 7.B - R_s value from excluded **flux** signal.

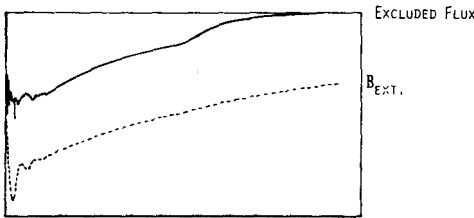


Fig.7.C - Signals from B_{ext} and $\Delta\phi$ excluded **flux** loops.

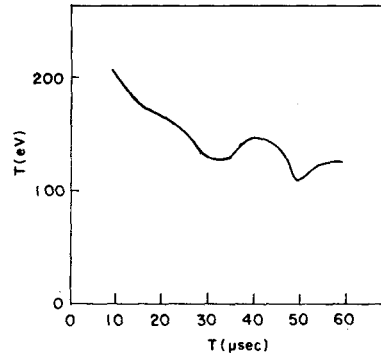


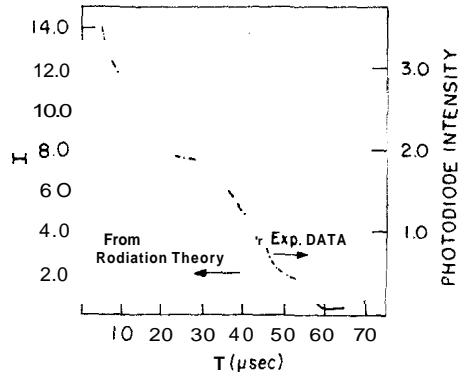
Fig. 7.D - $\langle T \rangle$ curve from $\langle \beta \rangle$ calculation.

Therefore if we accept the photodiode signal as being from **bremsstrahlung** radiation we can **estimate** the electron temperature with the equation

$$T_e = \left(\frac{I_{photo}}{A n^2 r_s} \right)^2 \quad (5)$$

As before, the **density** is obtained from interferometric data and the **separatrix** radius r_s , from **flux** excluded probe. The constant A is a calibration constant

Fig.8 - Curves from photodiode and bremsstrahlung radiation theory.



to be determined for each setup with a **calibrated** source, or **else**, eq.(5) can be used to obtain the **relative** electron temperature in arbitrary units as seen in the fig. 9. This represents a very easy method to **estimate** the electron temperature, when compared with other techniques such as Thomson scattering, and gives more details than averaged **temperature** obtained from $\langle \beta \rangle$ value.

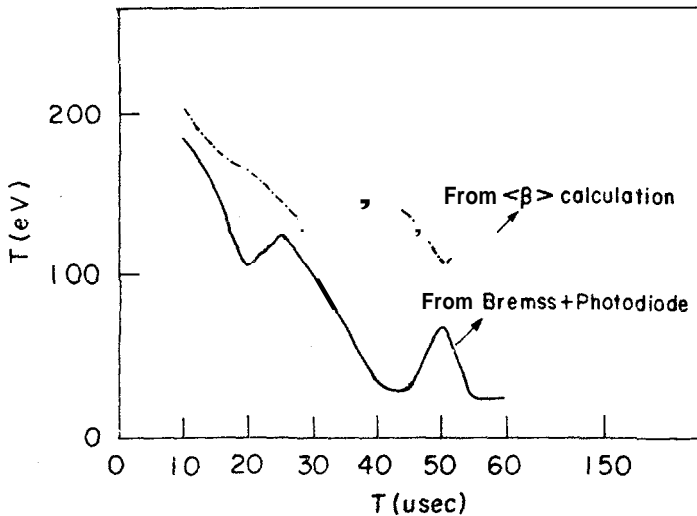


Fig.9 - Temperature obtained by $\langle \beta \rangle$ value (upper) and bremsstrahlung photodiode signal.

The angular velocity of the rotating plasma **column** can **also** be easily **deter-**mined using **two** photodiodes displaced by 45° on the radial plane. The result for

Photodiode measurements in Nucte-II

NUCTE-II is shown in fig. 1.0, which yields a velocity of 5×10^5 cm/s in the ion diamagnetic direction as seen also in other machines¹². Also the radial position of the plasma column and its length can be monitored by placing several diodes at suitable locations determined by shot to shot basis. The radial position of the column is monitored using three photodiodes displaced by 2.5 cm in the radial plane. The position is defined by the observation of the $n = 2$ instability for each channel. The results are shown in fig. 11, and indicate a quite well centered plasma column up to $45 \mu\text{s}$ into the discharge. The differences seen on the $n = 2$ instability at the center ($r = 0$ cm) and at $r = \pm 2.5$ cm, are due to the edge observations of elliptically deformed plasma.

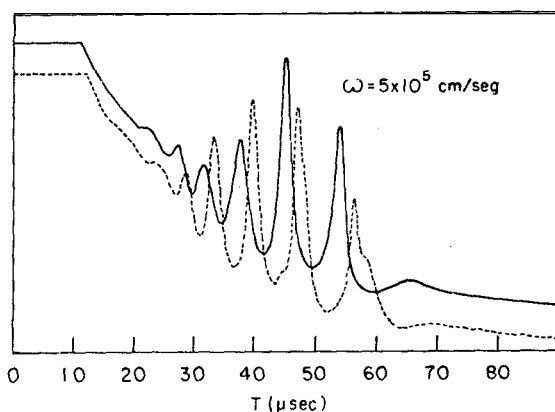


Fig.10 - Plasma rotation determined by instability signals taken with two radial 45° displaced photodiodes.

The length of the column is monitored with three diodes, at $z = +80.0$ cm, $z = 0$ cm and $z = -80.0$ cm. The results are shown in fig. 12. Again the final position has been obtained by shot to shot basis by monitoring the $n = 2$ instability. The plasma column length is found to be around 150 cm, shifted slightly to the left side; also, that plasma rotation appears earlier at the extremes of the column, leading to the speculation of a shear in the angular velocity, probably associated with a density profile in the z -direction.

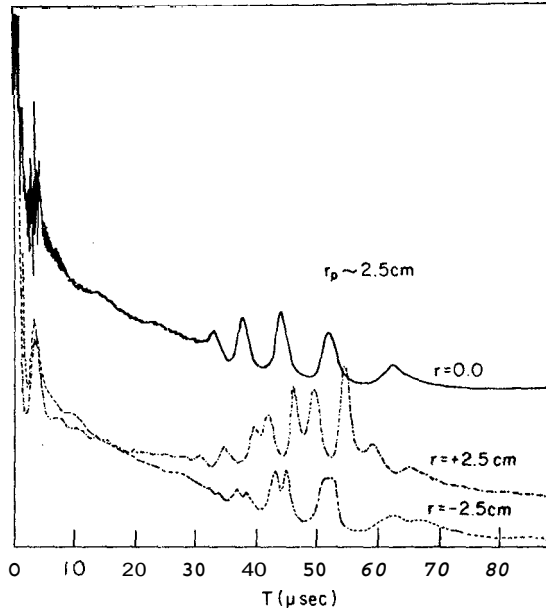


Fig. 11 - Signals from three radially displaced photodiodes for $Z=0.0$.

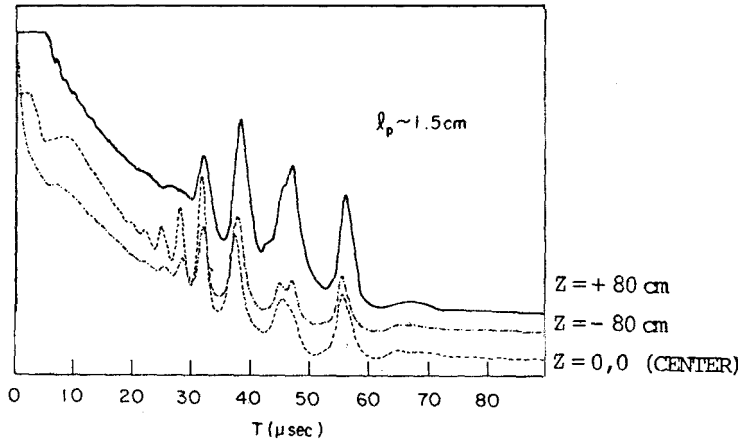


Fig.12 - Signals from three axially displaced photodiodes for $R=0.0$.

3. Conclusion

We have shown that the light detected by the photodiode is radiated from the

Photodiode measurements in Nuclte-II

whole plasma body and displays the characteristics of **bremsstrahlung** radiation. The detected intensity then can be used to determine the **relative** electron temperature as a function of time where the absolute calibration procedures, not used here, are necessary for more **accurate** temperature measurements. The detected signals agree very **well** with those obtained with laser interferometry. Appropriate positioning of **several diodes** allows an **unambiguous** determination of **the** rotation of the column and its angular velocity. The radial **and axial** displacements of the plasma **column** during the discharge **also** can be monitored with **this** technique.

References

1. W.T. Armstrong, R.K. Linford, J. Lipson, D.A. Platts and E.G. Sherwood, Phys. Fluids 24, **2068 (1981)**.
2. D.C. Barnes, W.T. Armstrong, E.J. Caramana, R.E. Chrien, W.N. Hugrass, H.R. Lewis, R.K. Linford, K.M. Ling, K.F. Mackenna, D.J. Rej, D.S. Harned, S. Okada, C.E. Seyler, D.E. **Sumaker**, H. Tuzcek, G. Uloses, R.D. Brooks, Z.A. Pietrzyk, **K.D.** Hahn, D. Lotz, R. Ramen, J. Wight, Plasma Physics and Controlled Nuclear Fusion Research – Nuclear Fusion Supplement, **vol.2**, 673 (1987)
3. D.J. Rej, W.T. Armstrong, G.A. Barnes, R.E. Chrien, W.N. Hugrass, P.L. Klinger, K.F. Mckenna, R.E. Siemon, M. Tuszewski, Phys. Fluids 29, **2648 (1986)**.
4. S. Ohi, T. **Minato**, Y. Kawakami, M. Tanjyo, S. Okada, Y. Ito, M. Kako, S. **Gotô**, T. Ishimura, H. **Itô**, Phys. Rev. Lett., **51**,1042(1983).
5. T. Ishimura, Phys. Fluids 27, **2139 (1984)**.
6. **Y.** Ito, **K.** Tsukuda, S. Goto, T. Ishimura, J. Appl. Phys. **58**, 1752 (1985).
7. S. Shimamura, **Y.** Nogi, Fusion Technologi 9, **69 (1986)**.
8. A. Vannucci, **Ph.D.** Thesis, I/F.-USP (1987).
9. I.H. Tan, **MS.** Thesis, I/F.-USP (1984).
10. J. Sheffield, Plasma Scattering of Electromagnetic Radiation Academic Press (1975).

11. S. Okada, Y. Ito, M. Kako, R.E. Chrien, S. Ohi, S. Goto, T. Ishimura, H. Itô, T. Takahashi, M. Ohara, S. Shimamura, M. Machida, Y. Nogi, Plasma Physics and Controlled Nuclear Fusion **Research**, Nuclear Fusion Supplement, vol.2, 551 (1987).

Resumo

Utilizando um conjunto de detectores tipo fotodiodo foi analisada a luz emitida pelo plasma produzido em um theta-pinch de campo reverso **NUCTE-II**. A análise mostra que a emissão de luz pelo plasma pode ser relacionada com a radiação **bremsstrahlung** e isto pode ser utilizado para obter parâmetros da instabilidade rotacional $n = 2$ tais como direção de **rotação**, velocidade angular, deslocamentos **axiais** e longitudinais da coluna do plasma. A variação da temperatura eletrônica do plasma **também** foi obtida quando utilizado em conjunto com outros **diagnósticos** tais como interferometria com **laser** H-Ne e sondas de fluxo excluído.